Long wavelength TCF-based fluorescence probe for the detection of Alkaline Phosphatase in live cells

Lauren Gwynne[1], Adam C. Sedgwick[2], Jordan E. Gardiner[1], George T. Williams[1], Gyoungmi Kim[3], Jean-Yves Maillard[4], Toby Jenkins[1*], Steven D. Bull[1*], Jonathan L. Sessler[2*], Juyoung Yoon[3*], Tony D. James[1*]

[1]University of Bath, United Kingdom, [2]University of Texas at Austin, United States, [3]Ewha Womans University, South Korea, [4]Cardiff University, United Kingdom

Submitted to Journal:
Frontiers in Chemistry

Specialty Section:
Supramolecular Chemistry

Article type:
Original Research Article

Manuscript ID:
446203

Received on:
02 Jan 2019

Revised on:
17 Feb 2019

Frontiers website link:
www.frontiersin.org

Long wavelength TCF-based fluorescent probe for the detection of Alkaline Phosphatase in live cells

Lauren Gwynne[1], Adam C. Sedgwick[2], Jordan E. Gardiner[1], George T. Williams[1], Gyoungmi Kim[3], John P. Lowe[1], Jean-Yves Maillard[4], A. Toby A. Jenkins[1*], Steven D. Bull[1*], Jonathan L. Sessler[2*], Juyoung Yoon[3*] and Tony D. James[1*]

[1]Department of Chemistry, University of Bath, Bath, UK.

[2]Department of Chemistry, University of Texas at Austin, Austin, USA.

[3]Department of Chemistry and Nano Science, Ewha Womans University, Seoul, Korea.

[4]Cardiff School of Pharmacy and Pharmaceutical Sciences, Cardiff University, Cardiff, UK.

*** Correspondence:**
Tony D. James, Juyoung Yoon, Jonathan L. Sessler, Steven D. Bull, A. Toby A. Jenkins
T.D.James@bath.ac.uk, jyoon@ewha.ac.k, sessler@cm.utexas.edu, S.D.Bull@bath.ac.uk,
A.T.A.Jenkins@bath.ac.uk

Keywords: Reaction-based fluorescent probe$_1$, Alkaline Phosphatase$_2$, Cell Imaging$_3$

Abstract

A long wavelength TCF-based fluorescent probe (**TCF-ALP**) was developed for the detection of alkaline phosphatase (ALP). ALP-mediated hydrolysis of the phosphate group of **TCF-ALP** resulted in a significant fluorescence 'turn on' (58-fold), which was accompanied by a colorimetric response from yellow to purple. **TCF-ALP** was cell-permeable, which allowed it to be used to image ALP in HeLa cells. Upon addition of bone morphogenic protein 2, **TCF-ALP** proved capable of imaging endogenously stimulated ALP in myogenic murine C2C12 cells. Overall, TCF-ALP offers promise as an effective fluorescent/colorimetric probe for evaluating phosphatase activity in clinical assays or live cell systems.

1 Introduction

Alkaline phosphatase (ALP) is an ubiquitous enzyme found in the majority of human tissues, where it catalyses the dephosphorylation of various substrates such as nucleic acids, proteins and other small molecules (Millán, 2006, Coleman, 1992). ALP also plays an important role in signal transduction and regulation of intracellular processes (cell growth, apoptosis and signal transduction pathways) (Julien et al., 2011). Abnormal levels of ALP in serum are an indicator of several diseases including bone disease (Garnero and Delmas, 1993), liver dysfunction (Rosen et al., 2016), breast and prostatic cancer (Ritzke et al., 1998, Wymenga et al., 2001) and diabetes (Tibi et al., 1988). As a result, ALP is regarded as a key biomarker in medical diagnosis (Coleman, 1992, Ooi et al., 2007). Therefore, it is important to develop a fast, reliable and selective detection system for monitoring ALP activity that is amenable to clinical diagnostics.

There have been numerous approaches to determine ALP levels, including colorimetric (Yang et al., 2016, Hu et al., 2017), chemiluminescent (Jiang and Wang, 2012), electrochemical (Zhang et al., 2015b), surface-enhanced Raman methods (Ruan et al., 2006) and fluorescence (Cao et al., 2016, Fan

et al., 2016). This work focused on the development of fluorescent probes for the detection of biologically relevant analytes (Sedgwick et al., 2017a, Sedgwick et al., 2018b, Wu et al., 2017, Sedgwick et al., 2017b, Sedgwick et al., 2018a, Zhang et al., 2019). Fluorescence has many advantages over other methods owing to its simplicity and high sensitivity/selectivity, providing rapid, non-invasive, real-time detection (Wu et al., 2017). Whilst there have been many fluorophores developed for assaying ALP activity such as organic dyes (Zhang et al., 2015a, Zhao et al., 2017), conjugated polymers (Li et al., 2014), inorganic semiconductor dots (Qian et al., 2015), and noble metal clusters (Sun et al., 2014), most require high probe concentrations and crucially rely on short wavelength emission, thus limiting their applicability in biological systems. Therefore, ALP probes that operate at long wavelengths are urgently required. Such probes should allow for deeper tissue penetration and be subjected to less cell-based autofluorescence (Liu et al., 2017, Zhang et al., 2017, Tan et al., 2017).

2 Results and Discussion

2.1 Chemistry

Here we report a TCF-based fluorescent probe that allows for the detection of ALP and/or ACP. As shown in **Scheme 1**, this probe (**TCF-ALP**) is based on the conjugation of 2-dicyanomethylene-3-cyano-4,5,5-trimethyl-2,5-dihydrofuran (**TCF**) to an electron-donating moiety, a phosphorylated phenol; this affords an internal charge transfer (ICT) donor-π-acceptor (D-π-A) system whose fluorescence properties vary dramatically following ALP-mediated phosphate group cleavage (Gopalan et al., 2004, Liao et al., 2006, Lord et al., 2008, Bouffard et al., 2008, Jin et al., 2010, Teng et al., 2018, Sedgwick et al., 2017b). **TCF-ALP** was synthesised in four steps with an overall yield of 27% (**Scheme 2**). In brief, 3-hydroxy-3-methyl-2-butanone, malononitrile and NaOEt were heated at reflux in EtOH for 1 h. The resultant precipitate **TCF (1)** was then treated with a mixture of piperidine (cat.) and 4-hydroxybenzaldehyde in EtOH to afford intermediate **2** (**TCF-OH**). Intermediate **2** was then treated with diethylchlorophosphate, DMAP (cat.) and NEt_3 in THF to give the phosphonate ester **3**. Hydrolysis using trimethylsilyl iodide in dichloromethane (DCM) afforded **TCF-ALP** as a crystalline solid (Et_2O).

2.2 Spectroscopic studies of TCF-ALP

UV-Vis and fluorescence spectroscopic titrations of **TCF-ALP** were performed in 50 mM Tris-HCl buffer in the absence and presence of ALP from porcine kidney. In the absence of ALP, **TCF-ALP** was found to have no UV absorption features above ~550 nm; however, upon addition of ALP a bathochromic shift in the UV absorption maximum was observed (from 440 to 580 nm), which was accompanied by a change in colour from yellow to purple (**Figure S1**). ALP-mediated hydrolysis of **TCF-ALP** to form highly fluorescent phenol (**2**), was confirmed by ^{31}P NMR studies and HRMS (See **Figure S1 – S4**). The effect of pH on the rate of ALP mediated hydrolysis of **TCF-ALP** was evaluated. It was found that incubation with 0.8 U/mL of ALP at pH 9.2 resulted in the largest fluorescence response (**Figure S5**). Consequently, all *in vitro* experiments to determine ALP activity were carried out in 50 mM Tris-HCl buffer at pH 9.2.

The kinetics of ALP towards **TCF-ALP** were determined *via* fluorescence spectroscopy (**Figure S6** and **S7**), with the resultant fluorescence data analysed using the Michaelis-Menten equation (**Figure S8**). This revealed a K_m of 35.81 ± 2.63 μM and a V_{max} of 3029 ± 157.3 min^{-1} for hydrolysis of **TCF-ALP** by ALP at pH 9.2 (see SI for details). **TCF-ALP** was then incubated with various concentrations of ALP (0.0 – 0.2 U/mL) for 15 minutes to evaluate its ability to monitor ALP activity. As shown in **Figure 1**, a significant fluorescence response was observed in the presence of ALP (58-fold) with a limit of detection (LOD) calculated as 0.12 mU/mL (**Figure S9**). This sensitivity is comparable to other

fluorescent probes found in literature (**Table S3**). Although serum alkaline phosphatase levels vary with age in normal individuals (Lowe et al., 2018), it is widely accepted that serum ALP levels in healthy adults lies between 39 – 117 U/mL (Sahran et al., 2018, Saif et al., 2005). This suggests that **TCF-ALP** is capable of detecting ALP in human serum, and therefore could be used in clinical assays.

Inhibition studies were carried out in the presence of sodium orthovanadate (Na_3VO_4), which is known to be a strong inhibitor of ALP activity. Addition of Na_3VO_4 resulted in a decrease in the fluorescence response in the **TCF-ALP** hydrolysis assay (see **Figure S10**) (Swarup et al., 1982). These inhibition studies enabled an IC_{50} of 6.23 µM to be calculated (**Figure S11**), which is similar in value to other ALP substrates that have been reported in the literature (Tan et al., 2017, Zhang et al., 2015a).

The selectivity of **TCF-ALP** towards other biologically relevant enzymes (at their optimal pH values) was then determined (**Figure 2** and **S12**), with **TCF-ALP** displaying high substrate selectivity for ALP over other common hydrolytic enzymes (e.g. trypsin, porcine liver esterase) or non-specific binding proteins (e.g. bovine serum albumin (BSA)). Interestingly, **TCF-ALP** produced a fluorescence response when treated with acid phosphatase (ACP). The detection of this enzyme is of significance since it is a tumour biomarker for metastatic prostate cancer (Makarov et al., 2009). Normal levels of ACP in serum range from 3.0 – 4.7 U/mL, and elevated ACP levels can be indicative of a variety of other diseases (Bull et al., 2002). Furthermore, **TCF-ALP** proved capable of detecting ACP (25-fold fluorescence enhancement) and ALP (38-fold enhancement) at a physiological pH of 7.1 (**Figure S13** and **S14**). Kinetic determination of ALP and ACP towards **TCF-ALP** at pH 7.1 was conducted, and the resultant K_m and V_{max} were compared (see SI **2.1** and **Figures S15-S18**). It was found that ALP has a smaller K_m value in comparison to ACP (0.38 ± 0.042 µM and 99.22 ± 13.16 µM respectively) and a lower V_{max} (208 ± 3.81 min^{-1} and 1962 ± 223.6 min^{-1} respectively). Hence, ALP has higher affinity towards **TCF-ALP** compared to ACP, thus is more selective towards ALP at physiological pH.

According to current standards, determination of ALP and ACP is undertaken at the phosphatase's optimum pH. For example, the Centers for Disease Control and Prevention (CDC) procedure for ALP determination is carried out in 2-amino-2-methyl-1-propanol (AMP) buffer at pH 10.3 ((CDC), 2012). This is in accordance with other literature sources (Guo et al., 2018, Di Lorenzo et al., 1991, Radio et al., 2006, Pandurangan and Kim, 2015). Likewise, ACP determination is carried out at pH 4-6 (Myers and Widlanski, 1993, Boivin and Galand, 1986, LI et al., 1984). Following these observations, further studies were conducted to determine selectivity at pH 5.0 and 9.2 (**Figures S19 – S22**). Results showed that **TCF-ALP** acts selectivity towards ACP at acidic pH, and ALP at alkaline pH. Therefore, **TCF-ALP** can be used to selectively detect ALP/ACP in clinical assays, or live cell systems (provided the buffer solution is optimal for the phosphatase under study).

2.3 Imaging of ALP in living cells

Prior to exploring whether **TCF-ALP** could be used to image ALP activity levels in live cells, the cytotoxicity of **TCF-ALP** was assessed using a MTT assay (**Figure S23**). Negligible cell toxicity was observed for **TCF-ALP** concentrations between 0 – 5 µM, and cell viability was only slightly reduced (91%) when incubated with 10 µM **TCF-ALP**, indicating good biocompatibility.

TCF-ALP proved cell permeable to HeLa cells that express ALP and provided a clear 'turn on' response (**Figure 3**). In contrast, pre-treatment of HeLa cells with 5 mM Na_3VO_4 prior to incubation with **TCF-ALP** resulted in minimal 'turn on'. This was taken as evidence that the increase in **TCF-ALP** fluorescence levels seen for HeLa cells in the absence of Na_3VO_4 is due to ALP activity. We thus conclude **TCF-ALP** is a probe that allows for the selective cellular imaging of ALP activity.

Bone morphogenetic protein 2 (BMP-2) is capable of inducing osteoblast differentiation into a variety of cell types (Guo et al., 2014, Wang et al., 2015) *via* pathways that result in increased ALP mRNA expression, leading to increased ALP activity (Kim et al., 2004). Treatment of myogenic murine C2C12 cells with **TCF-ALP** resulted in a low fluorescence intensity (low ALP levels) being observed (**Figure 4**); however, pre-treatment of these cells with BMP-2 (300 ng/mL, 3 days) resulted in a significant increase in **TCF-ALP**-derived fluorescence intensity (high ALP levels). Once again, pre-incubation with 5 mM Na_3VO_4 led to no fluorescence response being observed in the cells treated with **TCF-ALP** (with or without BMP-2). This provided support for the notion that **TCF-ALP** is capable of imaging endogenous ALP activity induced by BMP-2.

3 Conclusions

In summary, a long wavelength TCF-based fluorescent probe (**TCF-ALP**) has been prepared with the goal of detecting ALP activity. ALP hydrolyses the phosphate group of **TCF-ALP** resulted in a significant 'turn on' fluorescence response (58-fold) within 15 minutes. These spectroscopic changes were accompanied by a colorimetric change from yellow to purple. This enables **TCF-ALP** to be used as a simple assay for the evaluation of ALP activity. Further analysis revealed that **TCF-ALP** could also be used as a probe for detecting ACP activity. **TCF-ALP** was shown to be cell permeable, enabling its use as a fluorescent probe for monitoring ALP levels in HeLa cells. **TCF-ALP** also proved capable of imaging endogenously stimulated ALP produced in myogenic murine C2C12 cells through the addition of bone morphogenetic protein 2. We thus suggest that **TCF-ALP** offers promise as a tool for measuring ALP and ACP activity levels in clinical assays or in live cell systems.

4 Conflict of Interest

The authors declare that the research was conducted in the absence of any commercial or financial relationships that could be construed as a potential conflict of interest.

5 Author Contributions

LG and ACS carried out synthetic and spectroscopic experiments and co-wrote the manuscript with TDJ and JLS. JEG and GTW carried out background experiments. GK carried out cellular imaging experiments. JPL carried out the ^{31}P NMR titrations. J-YM and ATAJ are supervisors of LG and GTW. SDB, JY, JLS and TDJ both conceived the idea and helped with the manuscript.

6 Funding

This work was supported in part by grant MR/N0137941/1 for the GW4 BIOMED DTP, awarded to the Universities of Bath, Bristol, Cardiff and Exeter from the Medical Research Council (MRC)/UKRI We would also like to thank the EPSRC (EP/R003939) and the University of Bath and Public Health England for funding. ACS and JLS thank The Robert A. Welch Foundation (F-0018).

7 Acknowledgments

TDJ wishes to thank the Royal Society for a Wolfson Research Merit Award. The EPSRC UK National Mass Spectrometry Facility at Swansea University is thanked for mass analyses.

8 Supplementary Material

Data supporting this study are provided as supplementary information accompanying this paper, which is available free of charge.

9 References

Boivin, P., and Galand, C. 1986. The human red cell acid phosphatase is a phosphotyrosine protein phosphatase which dephosphorylates the membrane protein band 3. *Biochem. Biophys. Res. Commun.,* 134**,** 557-564.

Bouffard, J., Kim, Y., Swager, T. M., Weissleder, R. and Hilderbrand, S. A. 2008. A highly selective fluorescent probe for thiol bioimaging. *Org. Lett.,* 10**,** 37-40.

Bull, H., Murray, P. G., Thomas, D., Fraser, A. M. and Nelson, P. N. 2002. Acid phosphatases. *J. Clin. Pathol. Molecular Pathology.* 55**,** 65-72.

Cao, F.-Y., Long, Y., Wang, S.-B., Li, B., Fan, J.-X., Zeng, X. and Zhang, X.-Z. 2016. Fluorescence light-up aie probe for monitoring cellular alkaline phosphatase activity and detecting osteogenic differentiation. *J. Mater. Chem. B,* 4**,** 4534-4541.

Centers For Disease Control and Prevention 2012. *Alkaline Phosphatase (ALP) in Refigerated Serum: NHANES 2011-2012.* Available: https://wwwn.cdc.gov/nchs/data/nhanes/2011-2012/labmethods/biopro_g_met_alkaline_phosphatase.pdf [Accessed 29/01/19.]

Coleman, J. E. 1992. Structure and mechanism of alkaline phosphatase. *Annu. Rev. Biophys. Biomol. Struct.,* 21**,** 441-483.

Di Lorenzo, D., Albertini, A., and Zava, D. 1991. Progestin regulation of alkaline phosphatase in the human breast cancer cell line T47D. *Cancer research,* 51**,** 4470-4475.

Fan, C., Luo, S. and Qi, H. 2016. A Ratiometric Fluorescent Probe For Alkaline Phosphatase Via Regulation Of Excited-State Intramolecular Proton Transfer. *Luminescence,* 31**,** 423-427.

Garnero, P. and Delmas, P. D. 1993. Assessment of the serum levels of bone alkaline phosphatase with a new immunoradiometric assay in patients with metabolic bone disease. *J. Clin. Endocrinol. Metab.,* 77**,** 1046-1053.

Gopalan, P., Katz, H. E., Mcgee, D. J., Erben, C., Zielinski, T., Bousquet, D., Muller, D., Grazul, J. and Olsson, Y. 2004. Star-shaped azo-based dipolar chromophores: design, synthesis, matrix compatibility, and electro-optic activity. *J. Am. Chem. Soc.,* 126**,** 1741-1747.

Guo, F., Jiang, R., Xiong, Z., Xia, F., Li, M., Chen, L. and Liu, C. 2014. Ire1a constitutes a negative feedback loop with bmp2 and acts as a novel mediator in modulating osteogenic differentiation. *Cell death dis.,* 5**,** e1239.

Guo, J., Gao, M., Song, Y., Lin, L., Zhao, K., Tian, T., Liu, D., Zhu, Z., and Yang, C. 2018. An allosteric-probe for detection of alkaline phosphatase activity and its application in immunoassay. *Front. Chem.,* 6**,** 618.

Hu, Q., Zhou, B., Dang, P., Li, L., Kong, J. and Zhang, X. 2017. Facile colorimetric assay of alkaline phosphatase activity using fe (ii)-phenanthroline reporter. *Chim. Acta,* 950**,** 170-177.

Jiang, H. and Wang, X. 2012. Alkaline phosphatase-responsive anodic electrochemiluminescence of cdse nanoparticles. *Anal. Chem.,* 84**,** 6986-6993.

Jin, Y., Tian, Y., Zhang, W., Jang, S.-H., Jen, A. K.-Y. and Meldrum, D. R. 2010. Tracking bacterial infection of macrophages using a novel red-emission ph sensor. *Anal. Bioanal. Chem.,* 398**,** 1375-1384.

Julien, S. G., Dubé, N., Hardy, S. and Tremblay, M. L. 2011. Inside the human cancer tyrosine phosphatome. *Nat. Rev. Cancer,* 11**,** 35.

Kim, Y.-J., Lee, M.-H., Wozney, J. M., Cho, J.-Y. and Ryoo, H.-M. 2004. Bone morphogenetic protein-2-induced alkaline phosphatase expression is stimulated by dlx5 and repressed by msx2. *J. Biol. Chem.*

Li, H. C., Chernoff, J., Chen, L. B. and Kirschonbaum, A. 1984. A phosphotyrosyl-protein phosphatase activity associated with acid phosphatase from human prostate gland. *Eur. J. Biochem.* 138**,** 45-51.

Li, Y., Li, Y., Wang, X. and Su, X. 2014. A label-free conjugated polymer-based fluorescence assay for the determination of adenosine triphosphate and alkaline phosphatase. *New J. Chem.,* 38**,** 4574-4579.

Liao, Y., Bhattacharjee, S., Firestone, K. A., Eichinger, B. E., Paranji, R., Anderson, C. A., Robinson, B. H., Reid, P. J. and Dalton, L. R. 2006. Antiparallel-aligned neutral-ground-state and zwitterionic chromophores as a nonlinear optical material. *J. Am. Chem. Soc.,*128**,** 6847-6853.

Liu, H.-W., Hu, X.-X., Zhu, L., Li, K., Rong, Q., Yuan, L., Zhang, X.-B. and Tan, W. 2017. In vivo imaging of alkaline phosphatase in tumor-bearing mouse model by a promising near-infrared fluorescent probe. *Talanta,* 175**,** 421-426.

Lord, S. J., Conley, N. R., Lee, H.-L. D., Samuel, R., Liu, N., Twieg, R. J. and Moerner, W. 2008. A photoactivatable push− pull fluorophore for single-molecule imaging in live cells. *J. Am. Chem. Soc.,* 130**,** 9204-9205

Lowe, D., John, S., Kent, K. and Rebedew, D. 2018. Alkaline phosphatase. *StatPearls*.

Makarov, D. V., Loeb, S., Getzenberg, R. H. and Partin, A. W. 2009. Biomarkers for prostate cancer. *Ann. Rev. Med,* 60**,** 139-151.

Millán, J. L. 2006. Alkaline phosphatases. *Purinergic signal.,* 2**,** 335.

Myers, J. K. and Widlanski, T. S. 1993. Mechanism-based inactivation of prostatic acid phosphatase. *Science,* 262**,** 1451-1453.

Ooi, K., Shiraki, K., Morishita, Y. and Nobori, T. 2007. High-molecular intestinal alkaline phosphatase in chronic liver diseases. *J. Clin. Lab. Anal.,* 21**,** 133-139.

Pandurangan, M. and Kim, D. H. 2015. ZnO nanoparticles augment ALT, AST, ALP and LDH expressions in C2C12 cells. *Saudi. J. Biol. Sci.,* 22**,** 679-684.

Qian, Z., Chai, L., Tang, C., Huang, Y., Chen, J. and Feng, H. 2015. Carbon quantum dots-based recyclable real-time fluorescence assay for alkaline phosphatase with adenosine triphosphate as substrate. *Anal. Chem.,* 87**,** 2966-2973.

Radio, N. M., Doctor, J. S. and Witt-Enderby, P. A. 2006. Melatonin enhances alkaline phosphatase activity in differentiating human adult mesenchymal stem cells grown in osteogenic medium via MT2 melatonin receptors and the MEK/ERK (1/2) signaling cascade. *J. Pineal Res.,* 40**,** 332-342.

Ritzke, C., Stieber, P., Untch, M., Nagel, D., Eiermann, W. and Fateh-Moghadam, A. 1998. Alkaline phosphatase isoenzymes in detection and follow up of breast cancer metastases. *Anticancer Res.,* 18**,** 1243-1249.

Rosen, E., Sabel, A. L., Brinton, J. T., Catanach, B., Gaudiani, J. L. and Mehler, P. S. 2016. Liver dysfunction in patients with severe anorexia nervosa. *Int. J. Eat. Disord.,* 49**,** 151-158.

Ruan, C., Wang, W. and Gu, B. 2006. Detection of alkaline phosphatase using surface-enhanced raman spectroscopy. *Anal. Chem,* 78**,** 3379-3384.

Sahran, Y., Sofian, A. and Saad, A. 2018. Pre-treatment serum lactate dehydrogenase (LDH) and serum alkaline phosphatase (ALP) as prognostic factors in patients with osteosarcoma. *J Cancer. Prev. Curr. Res.,* 9**,** 58-63.

Saif, M. W., Alexander, D. and Wicox, C. M. 2005. Serum alkaline phosphatase level as a prognostic tool in colorectal cancer: a study of 105 patients. *J. Appl. Res,* 5**,** 88.

Sedgwick, A. C., Chapman, R. S. L., Gardiner, J. E., Peacock, L. R., Kim, G., Yoon, J., Bull, S. D. and James, T. D. 2017a. A bodipy based hydroxylamine sensor. *Chem. Commun.,* 53**,** 10441-10443.

Sedgwick, A. C., Gardiner, J. E., Kim, G., Yevglevskis, M., Lloyd, M. D., Jenkins, A. T. A., Bull, S. D., Yoon, J. and James, T. D. 2018a. Long-wavelength tcf-based fluorescence probes for the detection and intracellular imaging of biological thiols. *Chem. Commun.,* 54**,** 4786-4789.

Sedgwick, A. C., Han, H. H., Gardiner, J. E., Bull, S. D., He, X. P. and James, T. D. 2017b. Long-wavelength fluorescent boronate probes for the detection and intracellular imaging of peroxynitrite. *Chem. Commun.,* 53**,** 12822-12825.

Sedgwick, A. C., Han, H. H., Gardiner, J. E., Bull, S. D., He, X. P. and James, T. D. 2018b. The development of a novel and logic based fluorescence probe for the detection of peroxynitrite and gsh. *Chem. Sci.,* 9**,** 3672-3676.

Sun, J., Yang, F., Zhao, D. and Yang, X. 2014. Highly sensitive real-time assay of inorganic pyrophosphatase activity based on the fluorescent gold nanoclusters. *Anal. Chem.,* 86**,** 7883-7889.

Swarup, G., Cohen, S. and Garbers, D. L. 1982. Inhibition of membrane phosphotyrosyl-protein phosphatase activity by vanadate. *Biochem. Biophys. Res. Commun.,* 107**,** 1104-1109.

Tan, Y., Zhang, L., Man, K. H., Peltier, R., Chen, G., Zhang, H., Zhou, L., Wang, F., Ho, D. and Yao, S. Q. 2017. Reaction-based off–on near-infrared fluorescent probe for imaging alkaline phosphatase activity in living cells and mice. *ACS Appl. Mater. Interfaces,* 9**,** 6796-6803.

Teng, X., Tian, M., Zhang, J., Tang, L. and Xin, J. 2018. A tcf-based colorimetric and fluorescent probe for palladium detection in an aqueous solution. *Tetrahedron Lett.*.

Tibi, L., Collier, A., Patrick, A., Clarke, B. and Smith, A. 1988. Plasma alkaline phosphatase isoenzymes in diabetes mellitus. *Clin. Chim. Acta.,* 177**,** 147-155.

Wang, G., Zhang, X., Yu, B. and Ren, K. 2015. Gliotoxin potentiates osteoblast differentiation by inhibiting nuclear factor-κb signaling. *Ren. Mol. Med. Rep.,* 12**,** 877-884.

Wu, D., Sedgwick, A. C., Gunnlaugsson, T., Akkaya, E. U., Yoon, J. and James, T. D. 2017. Fluorescent chemosensors: the past, present and future. *Chem. Soc. Rev.,* 46**,** 7105-7123.

Wymenga, L., Boomsma, J., Groenier, K., Piers, D. and Mensink, H. 2001. Routine bone scans in patients with prostate cancer related to serum prostate-specific antigen and alkaline phosphatase. *BJU int.,* 88**,** 226-230.

Yang, J., Zheng, L., Wang, Y., Li, W., Zhang, J., Gu, J. and Fu, Y. 2016. Guanine-rich dna-based peroxidase mimetics for colorimetric assays of alkaline phosphatase. *Biosens. Bioelectron.,* 77**,** 549-556.

Zhang, H., Xiao, P., Wong, Y. T., Shen, W., Chhabra, M., Peltier, R., Jiang, Y., He, Y., He, J. and Tan, Y. 2017. Construction of an alkaline phosphatase-specific two-photon probe and its imaging application in living cells and tissues. *Biomaterials,* 140**,** 220-229.

Zhang, H., Xu, C., Liu, J., Li, X., Guo, L. and Li, X. 2015a. An enzyme-activatable probe with a self-immolative linker for rapid and sensitive alkaline phosphatase detection and cell imaging through a cascade reaction. *Chem. Commun.,* 51**,** 7031-7034.

Zhang, J., Chai, X., He, X.-P., Kim, H-J., Yoon, J. and Tian, H. 2019. Fluorogenic probes for disease-relevant enzymes. *Chem. Soc. Rev.,* 48**,** 683-722.

Zhang, L., Hou, T., Li, H. and Li, F. 2015b. A highly sensitive homogeneous electrochemical assay for alkaline phosphatase activity based on single molecular beacon-initiated t7 exonuclease-mediated signal amplification. *Analyst,* 140**,** 4030-4036.

Zhao, L., Xie, S., Song, X., Wei, J., Zhang, Z. and Li, X. 2017. Ratiometric fluorescent response of electrospun fibrous strips for real-time sensing of alkaline phosphatase in serum. *Biosens. Bioelectron.,* 91**,** 217-224.

10 Captions for Figures and Schemes

Scheme 1 – A TCF-based fluorescence probe (**TCF-ALP**) for the detection of alkaline phosphatase.

Scheme 2 – Synthesis of **TCF-ALP.**

Figure 1 - Fluorescence spectra of **TCF-ALP** (10 µM) produced via the addition of alkaline phosphatase (ALP; 0 – 0.2 U/mL) in 50 mM Tris-HCl buffer, pH = 9.2 at 25 °C. λ_{ex} = 542-15 nm. All measurements were made 15 min after the addition of ALP.

Figure 2 - Fluorescence spectra of **TCF-ALP** (10 µM) recorded in the presence of trypsin (0.8 BAEE U/mL), porcine liver esterase, protease from *Streptomyces griseus*, proteinase K, bovine serum albumin (0.1 mg/mL), acid phosphatase (50 mM Tris-HCl, pH = 5.0) and alkaline phosphatase (50 mM Tris-HCl, pH = 9.2). All enzymes were standardised to 0.8 U/mL in Tris-HCl buffer pH 7.1 unless otherwise stated. λ_{ex} = 542-15 nm/ λ_{em} = 606 nm. Fluorescence measurements were made 30 min after adding the enzyme in question.

Figure 3 - HeLa cells incubated under the following conditions: (a) No treatment. (b) **TCF-ALP** (10 µM, 30 min). (c) Pre-treated with Na_3VO_4 (5 mM, 30 min), followed by the addition of **TCF-ALP** (10 µM, 30 min). (d) Pretreated with Na_3VO_4 (0.5 mM, 30 min) and **TCF-ALP** (10 µM, 30 min). Cells were washed with DPBS before their fluorescence images were acquired using a confocal microscope. Top half: fluorescence images, bottom half: fluorescence images merged with its corresponding DIC image. Ex. 559 nm/ em. 575-675 nm. Scale bar : 20 µm. DIC - differential interference contrast.

Figure 4- **TCF-ALP** in C2C12 cell. C2C12 cells were treated with 300 ng/mL BMP-2 for 3 days and then pretreated with 5 mM levamisole for 30 min and stained with 10 µM probe for 30 min. After washing with DPBS, fluorescence images were acquired by confocal microscopy. (a) only probe, (b) levamisole + probe, (c) BMP-2 + probe (d) BMP-2 + levamisole + probe. Top : fluorescence images, bottom : merged with DIC image. Ex. 559 nm/ em. 575-675 nm. Scale bar : 20 µm. DIC - differential interference contrast.

Figure 1.TIF

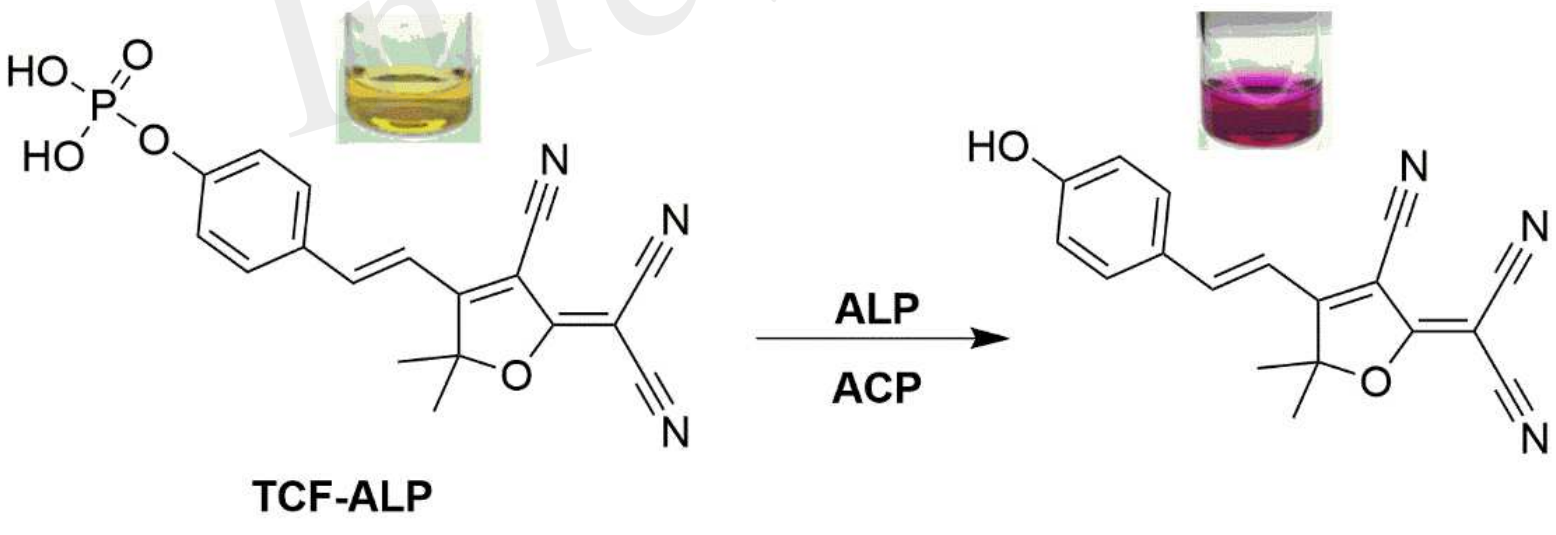

Figure 2.TIF

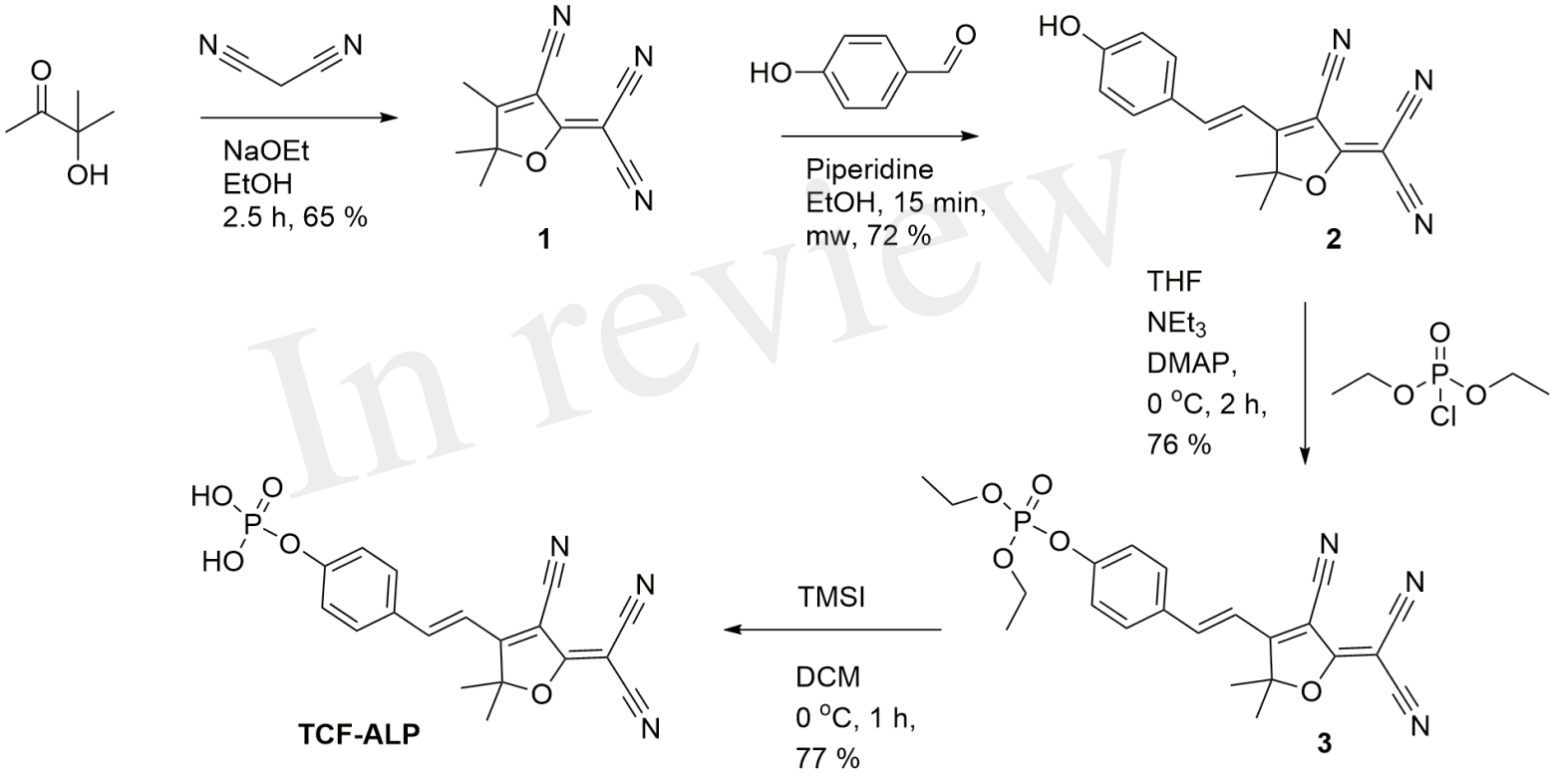

Figure 3.TIF

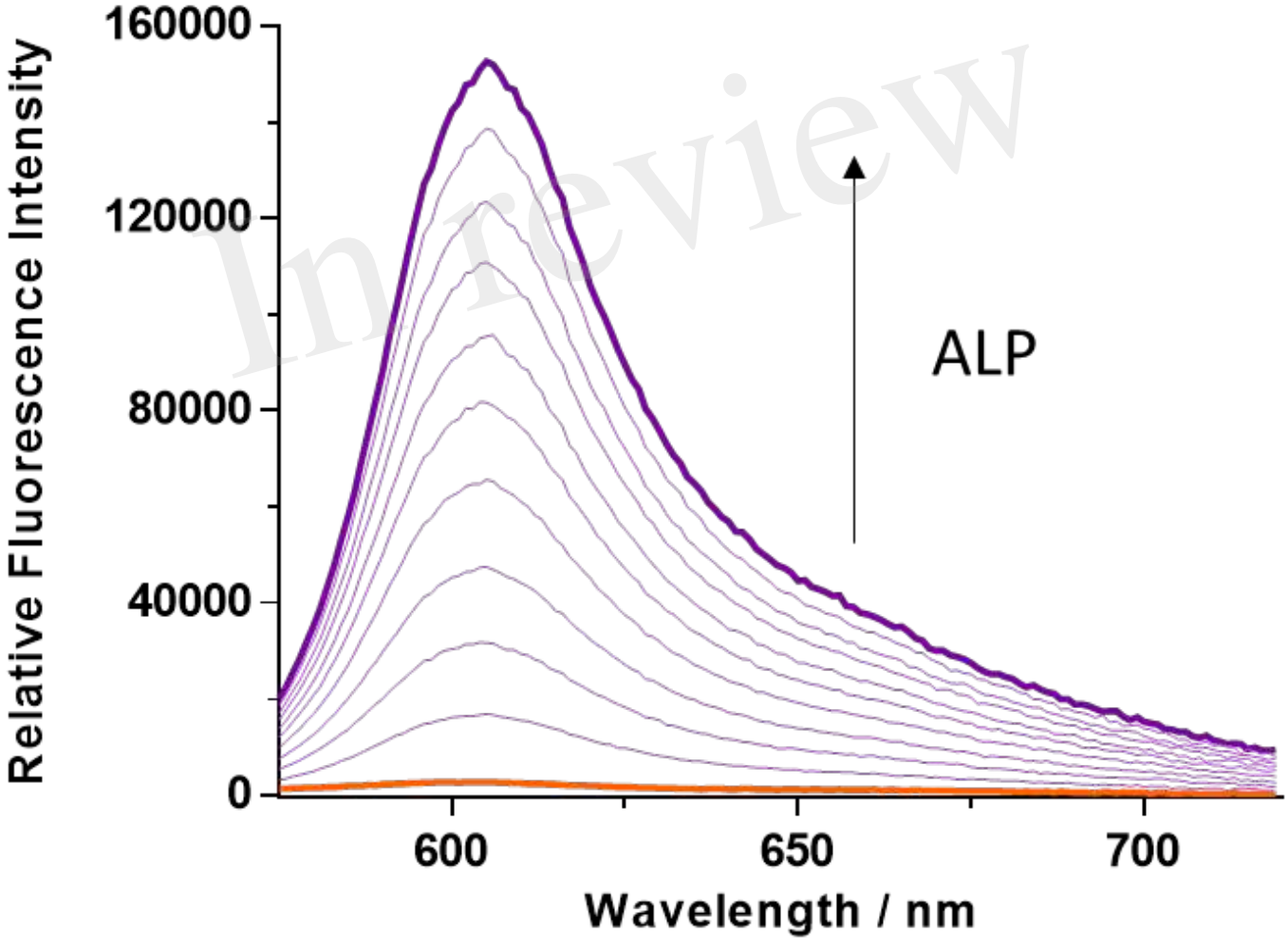

Figure 4.TIF

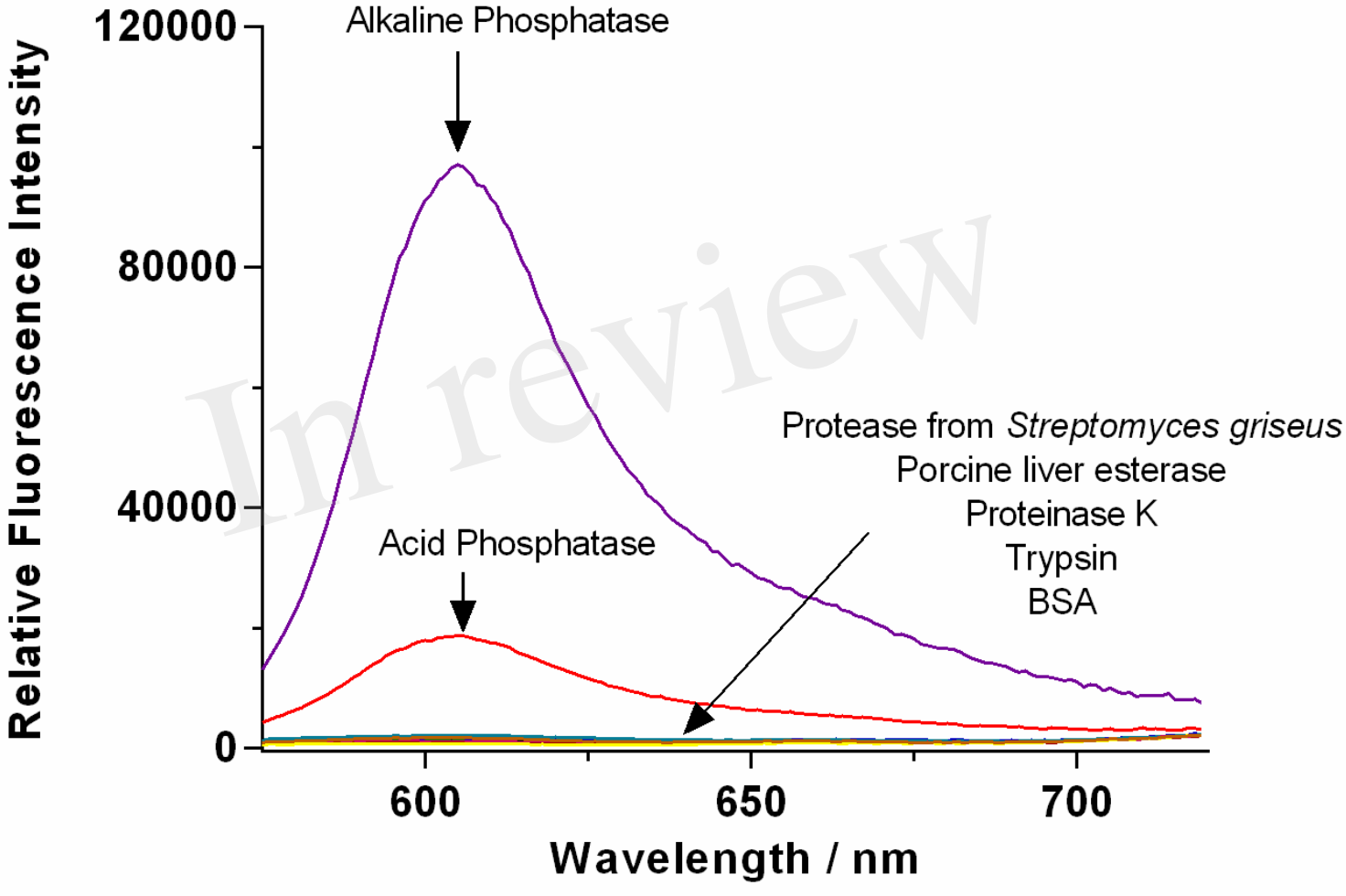

Figure 5.TIF

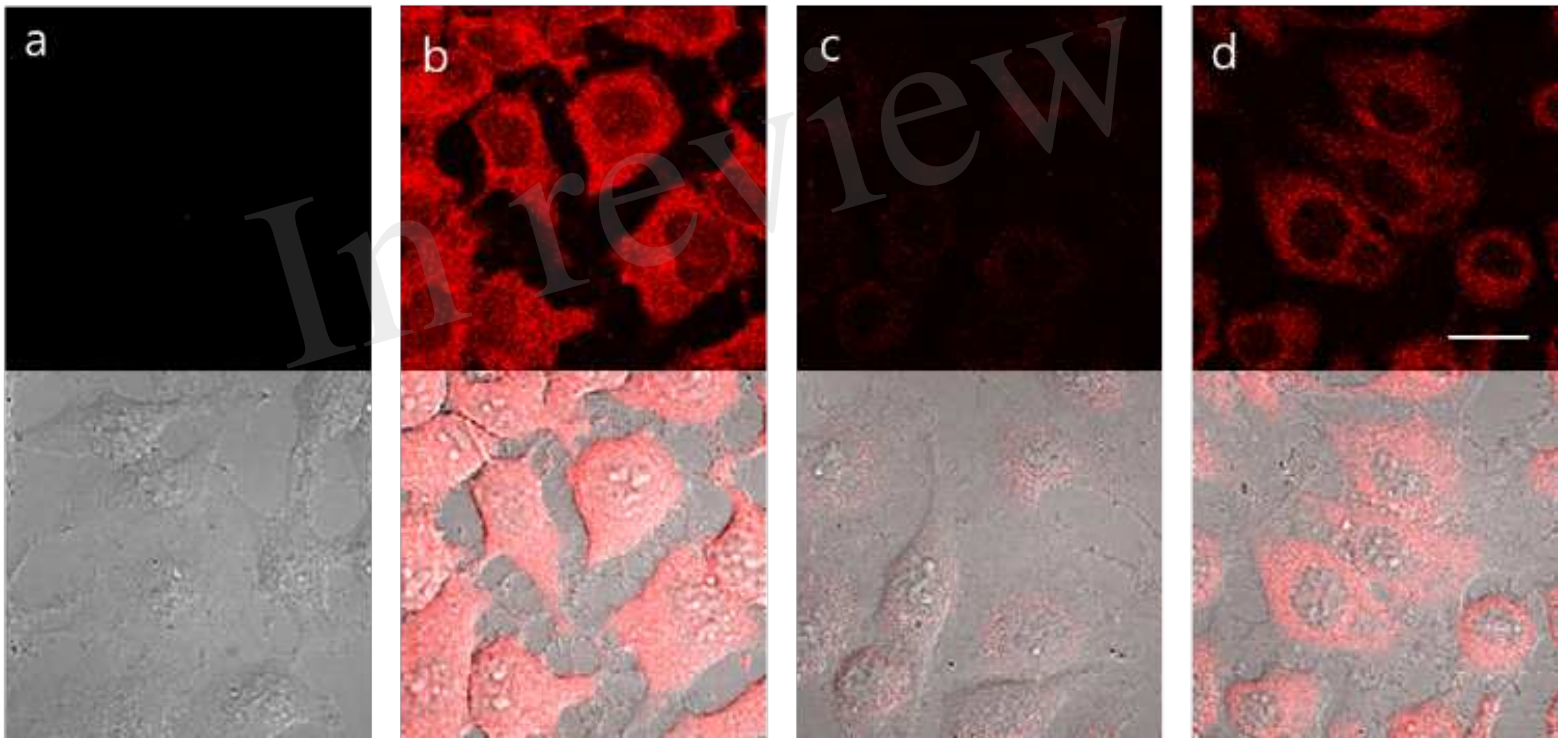

Figure 6.TIF